Constraining the symmetry term in the nuclear equation of state at subsaturation densities and finite temperatures

P. Marini,[1,*] A. Bonasera,[1,2] A. McIntosh,[1] R. Tripathi,[1,3] S. Galanopoulos,[1,†] K. Hagel,[1] L. Heilborn,[1,4] Z. Kohley,[1,4,‡] L. W. May,[1,4] M. Mehlman,[1,5] S. N. Soisson,[1,2] G. A. Souliotis,[1,6] D. V. Shetty,[1,§] W. B. Smith,[1] B. C. Stein,[1,2] S. Wuenschel,[1,4] and S. J. Yennello[1,4]

[1]*Cyclotron Institute, Texas A&M University, College Station, Texas 77843, USA*
[2]*Laboratori Nazionali del Sud, INFN, via Santa Sofia, 62, 95123 Catania, Italy*
[3]*Radiochemistry Division, Bhabha Atomic Research Center, Mumbai, India*
[4]*Chemistry Department, Texas A&M University, College Station, Texas 77843, USA*
[5]*Physics and Astronomy Department, Texas A&M University, College Station, Texas 77843, USA*
[6]*Laboratory of Physical Chemistry, Department of Chemistry, National and Kapodistrian University of Athens, 15771 Athens, Greece*

(Received 5 April 2011; revised manuscript received 7 February 2012; published 30 March 2012)

Methods of extraction of the symmetry energy (or enthalpy) coefficient to temperature ratio from isobaric and isotopic yields of fragments produced in Fermi-energy heavy-ion collisions are discussed. We show that the methods are consistent when the hot fragmenting source is well characterized and its excitation energy and isotopic composition are properly taken into account. The results are independent of the mass number of the detected fragments, which suggests that their fate is decided very early in the reaction.

DOI: 10.1103/PhysRevC.85.034617 PACS number(s): 21.65.Ef, 24.10.Pa, 05.70.Fh, 25.70.Mn

I. INTRODUCTION

In the past few years the importance of the symmetry energy term in the nuclear equation of state has stimulated a growing interest in isospin effects in nuclear reactions. Understanding the properties of asymmetric nuclear matter both at normal densities and at densities away from the saturation density has an important impact on the study of nuclear structure close to drip lines [1] and on the study of astrophysical processes [2].

Recent measurements of the giant dipole [3], pygmy dipole [4] and giant monopole [5] resonances in neutron-rich nuclei, neutron and proton emission [6], isospin diffusion [7], and fragment isotopic ratio [8,9] have provided initial constraints on the density dependence of the symmetry energy at subsaturation densities. Refinement of these measurements with both stable and rare isotope beams in the near future will provide further stringent constraints. New crucial experimental constraints on the symmetry energy at suprasaturation densities are expected from the recent measurement on neutron-proton elliptic flow performed at GSI [10]. Nevertheless, the conclusions are model dependent, different analysis methods provide different results, and a consistent description of all available experimental data employing one type of equation of state is still lacking.

In this work, among the experimental observables commonly used to explore the symmetry energy at subsaturation densities, we will concentrate on yield ratios of fragments produced in multifragmentation processes at Fermi energies. Different methods to extract the "symmetry energy" coefficient from this observable have been proposed. Among those, we will focus on three seemingly different approaches: isoscaling [11–16], m-scaling [17], and isobaric yield ratio method [18], and we will show that consistent experimental results can be extracted provided that the properties of the hot fragmenting source, such as its isospin composition and excitation energy, are properly taken into account. The paper is structured as follows: Sec. II briefly describes the three methods. Sections III and IV present the motivation that led to this work and the experimental apparatus, respectively. The importance of the source reconstruction and the results are presented in Secs. V and VI, respectively, while Sec. VII presents conclusions.

II. THEORETICAL BACKGROUND

The study of the multifragmentation process in violent heavy-ion collisions at Fermi energies is important for the investigation of the symmetry energy. During the multifragmentation process, which has been related to a nuclear phase transition [19–22], subsaturation density may be achieved [23]. Free energies play an important role in mixed-phase environments. Indeed, the isotopic distribution of fragments produced in such collisions is governed by the free energy at the pressure and temperature of the fragmenting source. Thus, by assuming that the fragment production is governed by a purely statistical process at constant temperature T and pressure P, the yield of a fragment, with N neutrons and Z protons, $Y(N, Z, T, P)$, can be related to the nuclear Gibbs free energy $G(N, Z, T, P)$ [14]:

$$Y(N, Z, T, P) = Y_0 A^{-\tau} \exp\left\{ -\frac{G(N, Z, T, P)}{T} + \frac{\mu_n}{T} N + \frac{\mu_p}{T} Z \right\}, \quad (1)$$

*pmarini@comp.tamu.edu
†Present address: Greek Army Academy, Department of Physical Science, Athens, Greece.
‡Present address: National Superconducting Cyclotron Laboratory, Michigan State University, East Lansing, Michigan 48824, USA.
§Present address: Physics Department, Western Michigan University, Kalamazoo, Michigan 49008, USA.

where Y_0 is a constant, μ_n and μ_p are the neutron and proton chemical potentials, respectively, and T is the temperature of the emitting source. The factor $A^{-\tau}$ originates from the entropy of the fragment, i.e., the Fisher entropy [24,25]. The use of the Gibbs free energy [26] depends on the validity of the assumption of fragment production via an equilibrium mechanism at constant pressure. Other assumptions, and therefore other thermodynamic state functions, could be used [27,28], but it is undoubtedly true that the true fragment production scheme requires a kinetic treatment. For instance, if the volume is kept constant (freeze-out hypothesis), then the Helmholtz free energy, $F(N, Z, T, V)$, should be used. This ambiguity casts some doubts on the derived quantity, i.e., symmetry energy or enthalpy.

Within a liquid-drop description, the nuclear free energy, $F(N, Z, T, V)$, can be parametrized as a sum of the bulk, surface, Coulomb, and symmetry free energy contributions. The symmetry energy term is usually expressed as [12,29]

$$E_{\rm sym}(N, Z, T, V) = C_{\rm sym}(T, V)\frac{(N-Z)^2}{A}, \tag{2}$$

where $C_{\rm sym}(T, V)$ is the symmetry energy coefficient, V is the volume, and $A = N + Z$. Similarly, starting from the Gibbs free energy, $G(N, Z, T, P)$, the symmetry enthalpy term could be expressed by introducing a symmetry enthalpy coefficient $C_{h\rm sym}$, depending on (T, P). The logic employed in this work, in which an equilibrium process at constant pressure is assumed [14], will lead to the extraction of the symmetry enthalpy. The assumption of a constant volume [12] would have led to the extraction of the symmetry energy. Experimentally, whether the equilibrium process takes place at constant pressure or volume (freeze-out hypothesis) is not determined, and therefore the ambiguity on the extracted quantity is retained. However, some estimates show that the difference between the two quantities should be small below the critical point of the phase transition [30]. Above it, the PV product becomes finite, and the two quantities might significantly differ. Nevertheless, in Ref. [27] it is shown that the canonical and grand-canonical ensembles predict similar results if one is only interested in the ratio of the population of two adjacent isotopes, on which we will focus in this work. Keeping in mind this ambiguity, from now on we will refer to the experimentally extracted quantity as the "symmetry energy."

We now give a brief review of the three methods that we will use in our experimental analysis.

It has often been experimentally observed that the ratio of the yields of a fragment with N neutrons and Z protons produced in two similar reaction systems with different neutron-to-proton ratios is exponential in N and Z [11–16]. In the grand-canonical approximation, using Eq. (1) this ratio can be written as

$$\begin{aligned} R_{21}(N, Z, T, P) &= \frac{Y_2(N, Z, T, P)}{Y_1(N, Z, T, P)} \\ &= \frac{Y_{0,2}}{Y_{0,1}} \exp\{[(\mu_{n,2} - \mu_{n,1})N \\ &\quad + (\mu_{p,2} - \mu_{p,1})Z]/T\} \\ &= C \exp(\alpha N + \beta Z), \end{aligned} \tag{3}$$

under the assumption that the thermodynamic state points of the two equilibrated sources in the two reactions are the same (where the indices 1 and 2 denote neutron-poor and neutron-rich systems, respectively). This relation, known as isoscaling, has been found to describe the measured ratios over a wide range of complex fragments and light particles rather well [12] and to be a phenomenon common to many different types of heavy-ion reactions [8,13,15,16,31,32]. This suggests that free energy components sensitive to the neutron-proton concentration differences play a key role in the fragment formation process.

Recently, the modified Fisher model of Ref. [24] has been used to interpret multifragmentation data and extract information on the symmetry energy [17,18,33]. In this model, the free energy per particle is modified as [33]

$$\Psi(m_f, A, T, H) \leftrightarrow \frac{G(N, Z, T, P) - \mu_n N - \mu_p Z}{A}, \tag{4}$$

where m_f $(= \frac{N-Z}{A})$ is the relative isospin asymmetry of the fragment. This is the Landau free energy. The ansatz here is that near a critical point all the dependencies of the free energy are contained in the order parameter m_f and its conjugate field H [17,33,34]. In principle, we do not need to specify whether the system is at constant volume or pressure, as before. Comparing to Eq. (1), we should notice that $\Psi(m_f, A, T, H)$ includes the neutron and proton chemical potentials. Within this approach, the ratio of the free energy per particle to the temperature near the critical point is described by the expansion [33–35]

$$\begin{aligned} \frac{\Psi(m_f, A, T, H)}{T} &= \frac{1}{2}am_f^2 + \frac{1}{4}bm_f^4 + \frac{1}{6}cm_f^6 \\ &\quad - \frac{H}{T}m_f + O\big(m_f^8\big). \end{aligned} \tag{5}$$

The parameters a, b, and c, which depend on T and ρ [33], are used for fitting. We stress here that the "external field" in our case might be attributed to the difference in neutron and proton chemical potentials of the source [17,34]. Indeed, in the limit where $\mu_p = -\mu_n$, combining Eqs. (4) and (5), we obtain $2H = \mu_n - \mu_p$. Other terms, such as the volume, surface, Coulomb, and pairing contributions, might be negligible near the phase transition, as suggested by experimental data [33].

An exponential dependence on m_f has been experimentally observed for the ratio, R_{21}, of the yields of a fragment (m_f, A) produced in two similar reactions with different neutron-to-proton ratios [17]. This scaling has been referred to as *m-scaling*, to distinguish it from the known isoscaling. Indeed, the fragment yield ratio between two systems at the same thermodynamic state point depends only on the external field H/T:

$$R_{21}(m_f, A, T, H) = C \exp\left(\frac{\Delta H}{T} m_f A\right), \tag{6}$$

where $\Delta H/T = H_2/T - H_1/T$. Comparing Eq. (3) and (6) and assuming that $\alpha = -\beta$, we obtain $\frac{\Delta H}{T} = \alpha$, as has been suggested in Ref. [17]. Ignoring the isospin-symmetry-breaking Coulomb effects is a reasonable approximation for light nuclei, since we will show that the $\alpha = -\beta$ relationship is approximately satisfied in our experimental data [33].

Following the statistical interpretation of the isoscaling with the Statistical Multifragmentation Model (SMM) [13] and with the expanding emitting source model [12], it has been proposed that the symmetry energy coefficient can be extracted from the measured isoscaling parameters through the approximate formula [12]

$$\frac{C_{\rm sym}(T)}{T} = \frac{\alpha}{4\Delta}. \tag{7}$$

The two models of Refs. [12,13] are based on different assumptions; therefore we restrain from stating explicitly the $C_{\rm sym}$ dependence on V or P, which is model dependent.

In the literature a variety of definitions of the quantity Δ has been proposed [12,14]. Among those we will focus on two commonly used expressions and on one recently suggested.

In the context of the SMM and the expanding emitting source model, Δ is the difference of the asymmetries of the equilibrated emitting sources, defined as [12]

$$\Delta_{\rm source} = \left[\left(\frac{Z}{A}\right)_1^2 - \left(\frac{Z}{A}\right)_2^2\right]. \tag{8}$$

In general, due to the phenomenon of fractionation, fragments may not have the same isospin ratio of the fragmenting source and this could affect the value of $C_{\rm sym}$ obtained from the isoscaling coefficient.

A study of the isospin fractionation and the isoscaling with Antisymmetrized Molecular Dynamics simulations [36] has shown a linear relation between α and $(Z/A)^2$ of fragments. The quantity Δ has then been expressed as

$$\Delta_{\rm liquid}(Z) = \left[\left(\frac{Z}{\langle A\rangle}\right)_1^2 - \left(\frac{Z}{\langle A\rangle}\right)_2^2\right], \tag{9}$$

where $Z/\langle A\rangle$ is the proton fraction of the most probable isotope for fragments of a given Z with $A > 4$ ("liquid part") [14].

More recently, Tripathi *et al.* [37] have shown, in an investigation of the nuclear phase transition using the Landau free energy approach, that the position of the central minimum of the free energy is related to the average isospin asymmetry of the fragments produced in each event, excluding neutrons and protons, $\overline{m_f}$. This suggests Δ may be written as

$$\Delta_{\langle m_f\rangle} = \left(\frac{1-\langle\overline{m_f}\rangle}{2}\right)_1^2 - \left(\frac{1-\langle\overline{m_f}\rangle}{2}\right)_2^2, \tag{10}$$

where $\langle\overline{m_f}\rangle$ is the event average of the fragment relative isospin asymmetry,

$$\langle\overline{m_f}\rangle = \frac{1}{N}\sum_{i=1}^{N}\left[\sum_{j=1}^{K}\frac{m_{f_j}}{K_i}\right], \tag{11}$$

where N is the number of events and K is the event multiplicity excluding neutrons and protons.

We would like to stress here that the definitions of Δ proposed in Eq. (8), (9), and (10) differ significantly. While Eq. (8) relates Δ to the characteristics of the two sources, Eqs. (9) and (10) express Δ as a function of the characteristics of the fragments. Moreover, Eq. (10), as opposed to Eq. (9), takes into account, event by event, the multiplicity in addition to the composition of the fragments. Since the determination of $C_{\rm sym}/T$ from scaling parameters depends on Δ, the correct determination of Δ is critical.

Recently, a different method to determine $C_{\rm sym}/T$ has been proposed that does not depend on the definition of Δ. Within the modified Fisher model [24] it has been shown that the isotope yield ratio between two isobars differing by 2 units in the neutron excess $I = N - Z$ and produced by the same source can be written as [18]

$$\begin{aligned} R(I+2, I, A, T, \rho) &= \frac{Y(I+2, A, T, \rho)}{Y(I, A, T, \rho)} \\ &= \exp\left\{\frac{W(I+2, A, T, \rho) - W(I, A, T, \rho) + (\mu_n - \mu_p)}{T}\right. \\ &\quad \left. + S_{\rm mix}(I+2, A) - S_{\rm mix}(I, A)\right\}, \end{aligned} \tag{12}$$

where $W(I, A, T, \rho)$ is the free energy of the cluster at temperature T, which in Ref. [18] was approximated by the generalized Weiszäcker-Bethe semiclassical mass formula [38,39], and $S_{\rm mix}(I, A)$ is the cluster mixing entropy. Apart the change of the notation for the free energy, we stress that a similar formula could be derived at constant pressure, and thus the ambiguity discussed above remains also in this case. Note that the variable I, introduced for consistency with Ref. [18], could be expressed as a function of the isospin asymmetry m_f as $I = m_f A$. The authors show that the symmetry energy coefficient to temperature ratio can be expressed as

$$\frac{C_{\rm sym}(T)}{T} \approx -\frac{A}{8}[\ln R(3, 1, A) - \ln R(1, -1, A) - \delta(3, 1, A], \tag{13}$$

where $\delta(3, 1, A)$ is the difference in the mixing entropies and can be neglected, being rather small compared to the other terms in Eq. (13) [18].

Equation (13) can be derived within a Landau free energy approach, which is used here to show that the dependence of $C_{\rm sym}/T$ on the source characteristics, contained in H/T, cancels out to first order. The yield of each fragment can be expressed as a function of its free energy per particle, F, as in Eq. (5). By neglecting $O(m^4)$ and choosing $I = 1, -1$, i.e., $m_1 = 1/A$ and $m_2 = -1/A$, and $I = 3, 1$, i.e., $m_1 = 3/A$ and $m_2 = 1/A$, the logarithm of the two yields ratio can be written as

$$\begin{aligned} \ln R(1, -1, A) &\approx 2A\frac{H}{T}\frac{1}{A}, \\ \ln R(3, 1, A) &\approx -A\left[\frac{1}{2}a\frac{8}{A^2} - 2\frac{H}{T}\frac{1}{A}\right], \end{aligned} \tag{14}$$

where $1/2a$, the fitting parameter defined in Eq. (5), is by definition $C_{\rm sym}/T$ [17,33,35,37]. The difference between the two relations, as in Eq. (13), cancels out the dependence on $\frac{H}{T}$, removing the dependence on the characteristics of the source.

We would like to stress here that the main difference between the first two methods of extracting $C_{\rm sym}/T$ and the third is that in the first two cases we are computing the yield ratios of the same fragment produced by two different

sources, while in the third case we consider different isobars produced by a common source. Therefore, in the first two cases the determination of $C_{\rm sym}/T$ requires an estimation of $\frac{\Delta H}{T}$, while in the third case the dependence on the source characteristics is removed by computing the difference of two yield ratios. However, the isobaric yield ratio method is dependent on the selected isobars and vulnerable to secondary decay effects. Isoscaling and m-scaling are less affected by secondary de-excitation effects, since they are removed, to first order, when taking the ratio of the yields of the same fragment produced in two sources. We will show that the three methods, which are consistent within the Landau free energy approach [18,29], give $C_{\rm sym}/T$ in good agreement. Moreover, the agreement of the results could suggest the method of determination of Δ.

III. MOTIVATION OF THE PRESENT WORK

In the present work, fragment yield data from quasiprojectile fragmentation in ^{64}Zn + ^{64}Zn, ^{70}Zn + ^{70}Zn, and ^{64}Ni + ^{64}Ni at 35 A MeV have been analyzed using the isoscaling, the m-scaling, and the isobaric yield ratio methods. There are three issues for the determination of the $C_{\rm sym}/T$ values in Eqs. (7) and (13): the importance of the experimental conditions, the effect of the secondary decay, and the method of determination of Δ.

In a previous work, Wuenschel *et al.* [40] have presented data from quasiprojectile fragmentation in ^{78,86}Kr + ^{58,64}Ni at 35 A MeV, showing an independence of the isoscaling-extracted $C_{\rm sym}/T$ values from the charge of the analyzed fragments. Stringent constraints were applied for a careful characterization of the source with a well-defined neutron (proton) concentration. The data were collected by a 4π charged-particle detector array.

In the works presented in [17,18,29], data for the reactions ^{64,70}Zn + ^{58,64}Ni, ^{64,70}Zn + ^{112,124}Sn, ^{64,70}Zn + ^{197}Au, ^{64,70}Zn + ^{232}Th, ^{64}Ni + ^{58,64}Ni, ^{64}Ni + ^{112,124}Sn, ^{64}Ni + ^{197}Au, ^{64}Ni + ^{232}Th at 40 A MeV analyzed with isoscaling, m-scaling, and isobaric yield ratio methods instead show a strong dependence of $C_{\rm sym}/T$ values on the charge of the analyzed fragment. The data were collected with a detector telescope placed at 20°. The telescope allowed the clear identification of typically 6–8 isotopes for atomic number Z up to $Z = 18$. In contrast to the experimental conditions of Wuenschel *et al.* [40], the information on the fragmenting source was not available and the angular coverage was limited ($15^\circ < \theta < 25^\circ$). Thus the yield of each isotope was evaluated by using a moving-source fit, selecting fragments produced in the fragmentation of the overlapping region of the two colliding nuclei.

It should be mentioned here that, if compression effects and/or higher order terms in Eq. (13) are important, the isoscaling and the isobaric yield ratio methods might produce different results. Moreover, a different beam energy and different colliding nuclei could access different densities, thereby providing complementary information. Thus investigations under precise experimental constraints for the source properties are necessary, which is one of the goals of this paper.

Furthermore, the observation of an increasing behavior of $C_{\rm sym}/T$ as a function of the fragment mass raises the question of the effects of the secondary decay process on the observables. Indeed, in previous works, excitation energies of the primary fragments estimated from the associated light-charged-particle multiplicities [41,42] suggest that effects of secondary evaporation could be important. Another possibility could be that we are really measuring an enthalpy rather than the internal symmetry energy and different nuclei could be emitted at different volumes.

The third issue is the expression of the quantity Δ that is used to extract $C_{\rm sym}/T$ from the isoscaling and m-scaling parameters. Indeed, while Δ from Eq. (8) has been widely used after its introduction [12], the study of the isospin fractionation suggests that the connection between $C_{\rm sym}/T$ and the scaling parameters should be found in the fragment isotopic asymmetry [Eqs. (9) and (10)]. Whether the event composition [Eq. (10)] or the average composition of each fragment [Eq. (9)] is more relevant is still an open question, which is specifically addressed in this work.

In this work we investigate the importance of the source reconstruction and the calculation of Δ by comparing the $C_{\rm sym}/T$ values obtained with the three different methods.

IV. THE EXPERIMENT

The experiment was performed at the Texas A&M University K500 Superconducting Cyclotron. Beams of ^{64}Zn, ^{70}Zn, and ^{64}Ni at 35 A MeV beam energy were impinged on ^{64}Zn, ^{70}Zn, and ^{64}Ni targets. The 4π NIMROD-ISiS array [44,45] was used for the detection of charged particles, obtaining isotopic resolution for $Z \leqslant 17$. The detector telescopes, arranged on 15 rings centered on the beam axis, were composed of one silicon detector backed by a CsI(Tl) crystal with photomultiplier tube (PMT) readout. Two telescopes per ring, referred to as Super Telescopes, made use of two silicon wafers in front of the CsI(Tl) crystal, in order to improve the isotopic resolution. The charged-particle array was housed inside the TAMU Neutron Ball [45], which measured the free neutron multiplicity.

The mass identification of fragments is essential for isospin physics analysis. For $Z \leqslant 2$, mass identification was performed by pulse shape discrimination of the CsI(Tl) signal. The ΔE-E method was used for $Z \geqslant 3$ on Si-Si and Si-CsI telescopes. In Fig. 1 the isotopic distributions of Be and Si are shown as examples. We can see that the global fit (red, solid curve) reproduces the overall spectrum well. The individual Gaussian fits (black, dashed curves) show the overlapping of the mass distributions for different isotopes. Particles were confidently assigned a mass if the contamination from neighbor isotopes was less than 5–10%. As evidenced by the figure, the mass determination efficiency decreases for large A near the upper limit of the electronics range. Further details on the mass identification procedures and on the experiment can be found in [43].

Particle and event selections were performed to select quasiprojectile fragmentation events. The quasiprojectile source was reconstructed by accepting in each event fragments

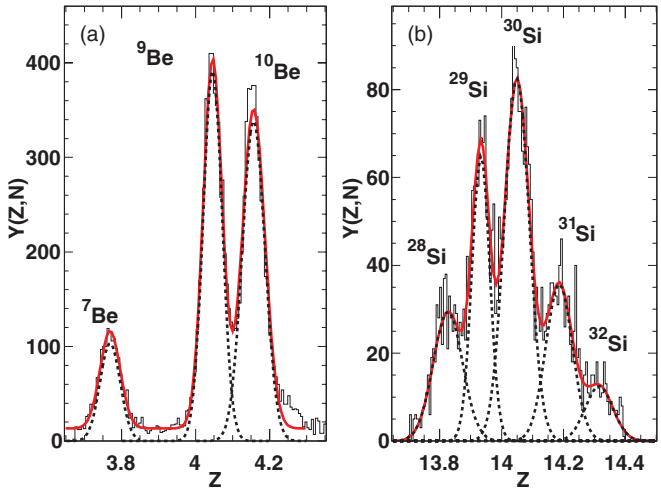

FIG. 1. (Color online) Isotopic distributions for $Z = 4$ (a) and $Z = 14$ (b) for a Super Telescope. The x axis is obtained by linearizing ΔE-E spectra as described in [43]. The Gaussian fits (black, dashed curves) show the overlapping of the mass distributions for different isotopes. The overall Gaussian fit is also shown (red, solid curves) for each Z.

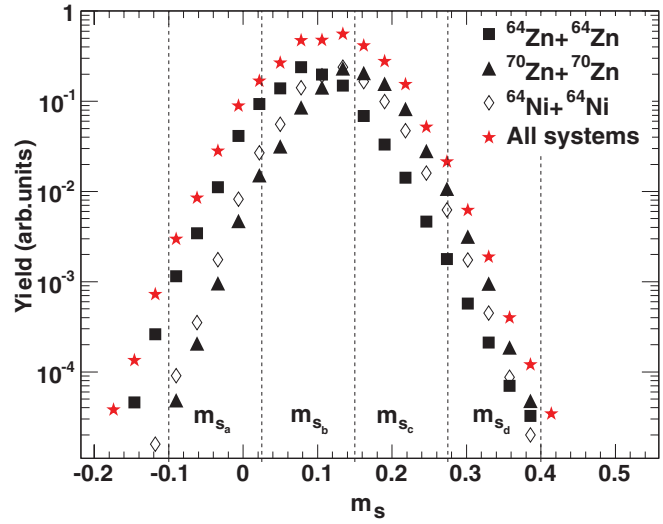

FIG. 2. (Color online) Reconstructed quasiprojectile m_s distribution from the ^{64}Zn + ^{64}Zn (squares), ^{64}Ni + ^{64}Ni (diamonds), and ^{70}Zn + ^{70}Zn (triangles) reactions. The total yield of each system was normalized to unity. The m_s distribution of the quasiprojectile obtained from the combined systems is plotted as stars. The total yield of this distribution was normalized to 3.

with a longitudinal velocity relative to the largest fragment within the range ±65%, ±60%, and ±45% for $Z = 1$, $Z = 2$, and $Z \geqslant 3$, respectively [46]. This cut, later referred to as *Vcut*, is intended to remove fragments from non-projectile-like sources. Furthermore, the total Z of the detected fragments included in the reconstruction was constrained to be in the range $Z = 25$–30 (*SumZ*). Finally, limits were placed on the deformation of the source, as measured by the quadrupole momentum, to select a class of events that are, on average, spherical. The quadrupole momentum, calculated from the measured particle momenta in the quasiprojectile frame, $\sum_i p_{\parallel_i}^2 / \sum_i p_{\perp_i}^2$, was required to be less than 2 (*Qcut*). Details on the source reconstructions can be found in Ref. [47]. Free neutrons measured by the Neutron Ball were used to correct for the free neutrons emitted by the quasiprojectile using the procedure discussed in Refs. [40,47].

V. IMPACT OF SOURCE RECONSTRUCTION

Figure 2 shows the distribution of the reconstructed quasiprojectile isospin asymmetry $m_s = \frac{N_s - Z_s}{A_s}$ for each of the three systems and for the three systems combined together. In the m_s expression, N_s, Z_s, and A_s are, respectively, the number of neutrons, protons, and total nucleons in the reconstructed quasiprojectile. As expected, the systems ^{70}Zn + ^{70}Zn and ^{64}Ni + ^{64}Ni, which have very similar N/Z values (1.33 and 1.29, respectively), show almost overlapping m_s distributions, with average values of $\overline{m_s} = 0.15$ and 0.13, respectively. The ^{64}Zn + ^{64}Zn m_s distribution is shifted toward lower m_s values ($\overline{m_s} = 0.09$), since the system is less neutron rich ($N/Z = 1.13$). The m_s distribution of the three combined systems is centered around $\overline{m_s} = 0.12$. The widths of the distributions are large compared to the difference in the average m_s between the reacting systems. In Ref. [40] it has been shown that an improved isoscaling can be obtained when selecting narrow bins in N/Z of the fragmenting source, rather than performing a system-to-system isoscaling. In analogy, and extending that work, we performed both isoscaling and m-scaling between two different m_s bins. For the isoscaling analysis using m_s, $\Delta\overline{m_s}$ refers to the difference of the mean m_s values in the two m_s bins. To allow a comparison of the results from the three different methods, for each m_s bin combination the isobaric yield ratio was computed for fragments produced by a source with $\langle m_s \rangle = \Delta\overline{m_s} \pm 0.0625$.

Fragment yield data were divided according to the relative isospin asymmetry, m_s, of the reconstructed source in four bins: $m_{s_a} = -0.0375 \pm 0.0625$, $m_{s_b} = 0.0875 \pm 0.0625$, $m_{s_c} = 0.2125 \pm 0.0625$, and $m_{s_d} = 0.3375 \pm 0.0625$, whose boundaries are also plotted in Fig. 2. The transverse excitation energy of the reconstructed source ($E_t^\star$) was calculated through calorimetry as [40,47]

$$E_t^\star = \sum_i^{M_{CP}} K_t^{CP}(i) + M_n \langle K_t^n \rangle - Q. \tag{15}$$

The first term is the sum of the transverse kinetic energies in the quasiprojectile center-of-mass frame of the particles (M_{CP}) belonging to the quasiprojectile (see Sec. IV, *VCut*). The free neutrons contribution to the excitation energy was estimated as the average neutron kinetic energy $\langle K_t^n \rangle$ multiplied by the neutron multiplicity M_n. The average transverse kinetic energy of the neutrons was calculated as the proton average transverse kinetic energy corrected for the Coulomb barrier energy [48]. The last term in the equation is the reaction Q value. The mass of the quasiprojectile was calculated as the sum of the masses of the charged particles belonging to the source and the neutron multiplicity. The transverse excitation energy per nucleon ($E_t^\star/A$) of the reconstructed source was calculated

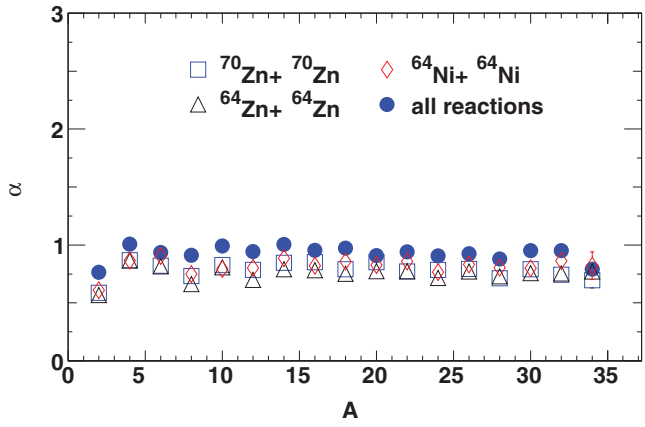

FIG. 3. (Color online) Isoscaling parameter α extracted for $\Delta\overline{m_s} = 0.185$ and $3.5 \leqslant E_t^\star/A \leqslant 5$ MeV from each reaction and for the combined systems as a function of the fragment mass ($A = 2Z$).

and the data were divided into five bins: $E_t^\star/A = (1.75 \pm 1.75)$, (4.25 ± 0.75), (5.75 ± 0.75), and (7.25 ± 0.75) MeV and $E_t^\star/A > 8$ MeV.

Figure 3 shows the isoscaling parameter α as a function of the mass fragment $A = 2Z$ extracted from each reaction (open symbols) and for the combined systems (full circles). The error bars are comparable to the size of the points. The isoscaling was performed between two sources with different m_s ($\overline{m_{s_1}} = -0.002$ and $\overline{m_{s_2}} = 0.183$) so that $\Delta\overline{m_s} = 0.185$. The source excitation energy was required to be between 3.5 and 5 A MeV. We observe that consistent α values for each mass were obtained for each system and for all the systems when the data were gated on m_s. The same results were obtained for all the m_s bin combinations and for all the excitation energies. Moreover, a similar behavior was observed for $\Delta H/T$ extracted from the m-scaling. Thus the systems were combined together to increase the statistics.

Significantly better isoscaling and m-scaling were obtained once two sources with different m_s rather than two different reactions were selected. In Fig. 4 the natural logarithm of the yield ratio of Eq. (3) and $\frac{1}{A}\ln R_{21}$ of Eq. (6) are plotted as a function of N and m_f, respectively. In Figs. 4(a) and 4(b) the ratios are computed between the yields of fragments produced in two different reactions (^{64}Zn + ^{64}Zn and ^{70}Zn + ^{70}Zn), while in Figs. 4(c) and 4(d) the fragments are produced by two sources with different m_s ($\overline{m_{s_1}} = 0.097$ and $\overline{m_{s_2}} = 0.180$), to construct the neutron-poor and the neutron-rich sources, as required from Eqs. (3) and (6). Comparison of these panels demonstrates the improvement of isoscaling and m-scaling with a narrowly defined m_s source. Indeed the isotopes line up on parallel, equally spaced lines in the isoscaling and on a single line in the m-scaling, as predicted by Eqs. (3) and (6), respectively.

To investigate the impact of the source reconstruction on the extracted values, the source constraints described in this and the previous sections have been imposed sequentially, on all the data, in order to illustrate the effect of each cut individually. The three methods have been applied to the so-selected data.

Figure 5 shows $\frac{C_{\rm sym}}{T}$, α, and $\Delta H/T$ extracted from the isobaric yield ratio [Eq. (13)], the isoscaling [Eq. (3)], and

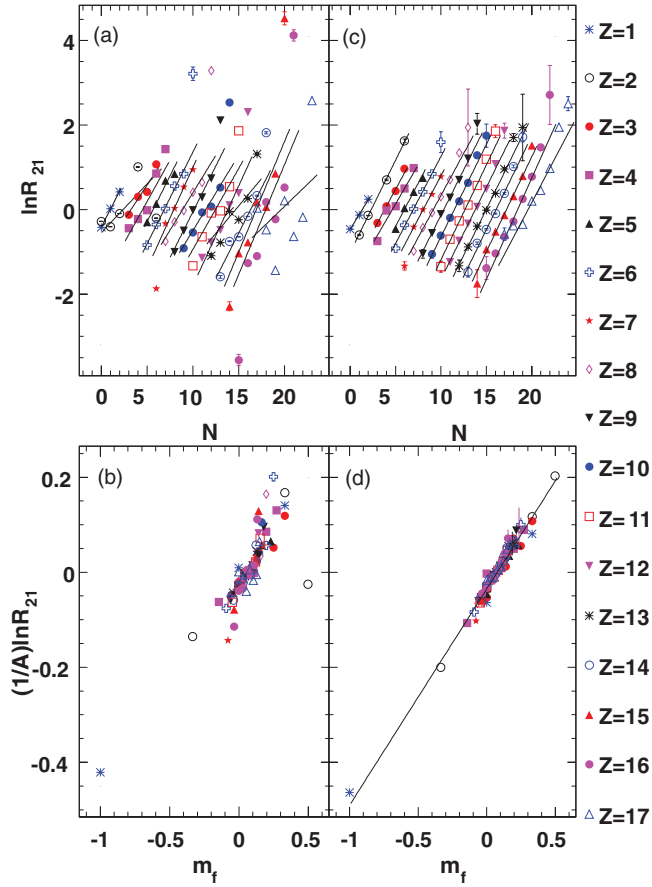

FIG. 4. (Color online) Natural logarithm of the isotopic yield ratio as a function of the fragment N [panels (a) and (c)] and natural logarithm of the isotopic yield ratio per fragment mass as a function of the fragment isospin asymmetry m_f [panels (b) and (d)]. Panels (a) and (b) show system-to-system isoscaling and m-scaling from ^{64}Zn + ^{64}Zn and ^{70}Zn + ^{70}Zn reactions. Panels (c) and (d) show isoscaling and m-scaling using different m_s bins of the reconstructed quasiprojectile (see text).

the m-scaling [Eq. (6)] methods, respectively, as a function of the fragment mass number A. For the x axis of the isoscaling and m-scaling methods $A = 2Z$. The α and $\Delta H/T$ parameters are both determined by individual fits to the yield ratios for isotopes with a given Z.

We first focus on the values obtained by comparing ^{70}Zn + ^{70}Zn to ^{64}Zn + ^{64}Zn systems (labeled as *SysToSys* in the figure), to analyze the impact of a limited angular coverage and of the quasiprojectile reconstruction. We will refer to these values as system-to-system values. A generally flat behavior is observed for α and $\Delta H/T$, independent of the fragment mass number A, when no constraints are imposed on the data (stars). The trends are modified neither by restricting our analysis to a limited angular range (diamonds) nor by selecting quasiprojectile fragmentation events (i.e., by applying *Vcut*, *SumZ*, and *QCut*-circles, triangles, and full squares, respectively). This suggests that the quasiprojectile selection does not significantly bias our determination of α or $\Delta H/T$.

In contrast to the flat behavior of the isoscaling and m-scaling, $\frac{C_{\rm sym}}{T}$ increases from 9 to 20 over the A range

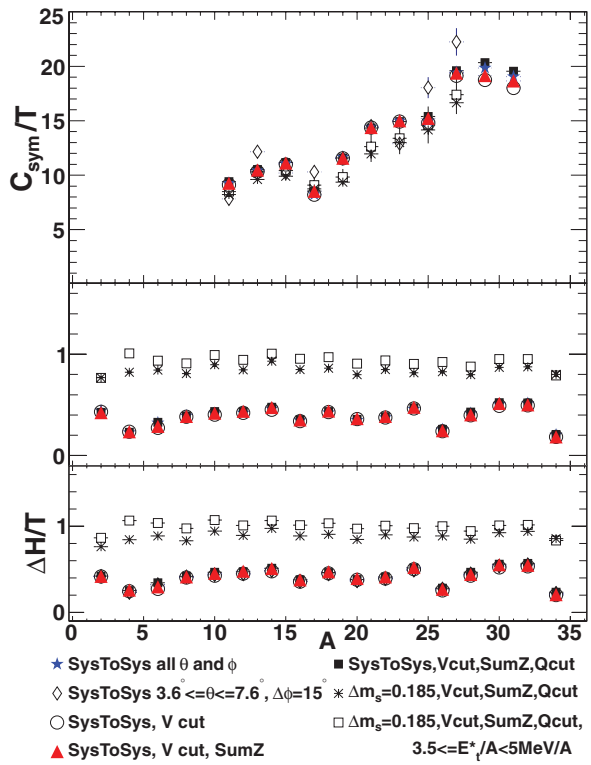

FIG. 5. (Color online) $\frac{C_{\rm sym}}{T}$, α, and $\frac{\Delta H}{T}$ obtained from isobaric yield ratio (top), isoscaling (middle), and m-scaling (bottom) methods, applied to two different reactions ("SysToSys") and two m_s bins (Δm_s). The source reconstruction constraints are applied to study their impact on the measured values. The error bars, when not visible, are comparable to the size of the symbols.

of 11 to 31, when no constraints are imposed on the data (stars). The increase is slightly amplified for $A = 25$ and 27 by selecting a limited angular range (diamonds) to simulate the angular coverage of Ref. [18]. The observed increase of 11 units in $\frac{C_{\rm sym}}{T}$ is similar to the one of 8 units reported in Ref. [18]. Data for masses $A > 27$ in a limited angular range are not available due to a statistics limitation. We should notice that the angular selection does not affect the values extracted from the isoscaling and m-scaling, since we take the ratio of the yields of the same fragment [Eqs. (3) and (6)]. This is not true for the isobaric yield ratio method, where different fragments considered in the calculation [see Eq. (12)] may be affected differently. To investigate the effect of a good resolution up to $Z = 18$, as in Ref. [18], we restricted the analysis to the detectors with the highest available resolution, the so-called Super Telescopes. Such a restriction does not modify the values of $\frac{C_{\rm sym}}{T}$, and therefore they are not plotted in the figure. Moreover, the selection of quasiprojectile fragmentation events does not modify the $\frac{C_{\rm sym}}{T}$ trend, as can be seen from the figure, since stars (no data selection), circles (*Vcut*), triangles (*Vcut* and *SumZ*), and full squares (*Vcut*, *SumZ*, and *Qcut*) overlap.

We turn now to analyze the impact of m_s (asterisks) and excitation energy (squares) constraints. The parameters α and $\Delta H/T$ are plotted for $\Delta\overline{m_s} = 0.185$, while $C_{\rm sym}/T$ has been obtained for $\langle m_s \rangle = 0.183$. The excitation energy was restricted to be between 3.5 and 5 A MeV. The behavior is flat, for both α and $\Delta H/T$, and presents less fluctuations with respect to the system-to-system values. The average value is 0.96 ± 0.01, to be compared to the system-to-system average value, 0.34 ± 0.01. The difference in the values observed is due to the different values of Δ in the two cases. Indeed, the values of Δ, determined as in Eq. (8) for isoscaling between two different systems and two different m_s bins, are 0.027 and 0.084, respectively, which give consistent values of α/Δ ($\alpha/\Delta = 12.6 \pm 0.4$ and 11.43 ± 0.12, respectively). The constancy of α/Δ was previously shown in [40].

A possible excitation energy dependence of α and $\Delta H/T$ is suggested by systematically higher (even if in agreement) α and $\Delta H/T$ values obtained for a selected source excitation energy (squares), compared to the ones obtained with no energy selection (asterisks). Indeed, the average excitation energy of the source in the latter case is higher (5.6 ± 1.6 A MeV) than the average excitation energy in the selected window (4.2 ± 0.4 A MeV). This trend is in agreement with the excitation energy dependence of the isoscaling parameter α/Δ observed for Kr + Ni systems in [40].

The selections in m_s and excitation energy do not modify the increasing trend of $\frac{C_{\rm sym}}{T}$ extracted by the isobaric yield ratio method. Though the values agree within statistical uncertainty, the m_s selection (asterisks and squares) results in a systematic lower $\frac{C_{\rm sym}}{T}$ for $A \geqslant 19$. A possible excitation energy dependence may be observed also in $\frac{C_{\rm sym}}{T}$ extracted by the isobaric yield ratio method. Indeed, for $A \geqslant 19$ the $\frac{C_{\rm sym}}{T}$ values obtained from data selected in excitation energy (squares) are very slightly higher than those obtained from data not selected in excitation energy (asterisks). Moreover, when performing an excitation energy selection we notice that different mass regions are populated depending on the source excitation energy: higher mass fragments ($A > 15$) are produced by low excited sources, while lower mass fragments ($9 \leqslant A \leqslant 15$) are mainly produced by highly excited sources. This is consistent with fragments being produced by different reaction mechanisms. Selection of heavy fragment multiplicity may weaken the dependence of $\frac{C_{\rm sym}}{T}$ on A. However, the present statistics do not allow this selection. These observations suggest that, in the absence of a source reconstruction, attention should be paid to mixing-reaction mechanisms when drawing general conclusions.

VI. COMPARISON OF THE THREE METHODS

The following analysis was performed by applying the described selections on the reconstructed quasiprojectile (see Sec. V for details). The quasiprojectiles were divided into bins based on their composition m_s and their excitation energy per nucleon.

The isoscaling parameters α and β were extracted simultaneously by a global fit to the yield ratios of all the available isotopes and, separately, by individual fits to the yield ratios for isotopes with a given Z. The obtained values were in good agreement. The parameter β shows the same trend as a function of N as α does as a function of Z, but it has the opposite sign.

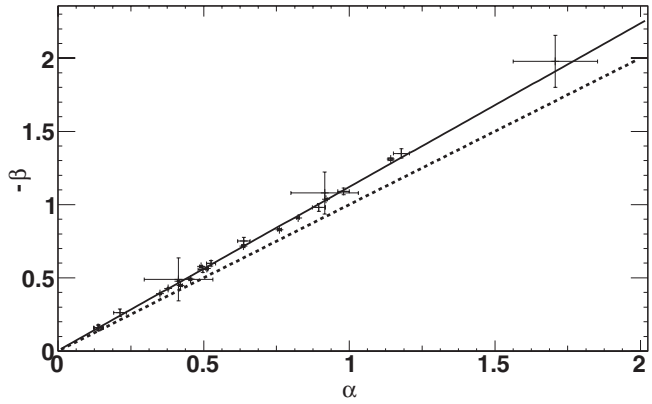

FIG. 6. Isoscaling parameters $-\beta$ vs α for all the $\Delta\overline{m_s}$ and excitation energy bins. The full line is the best fit to the data, while the dashed line represents $\alpha = -\beta$.

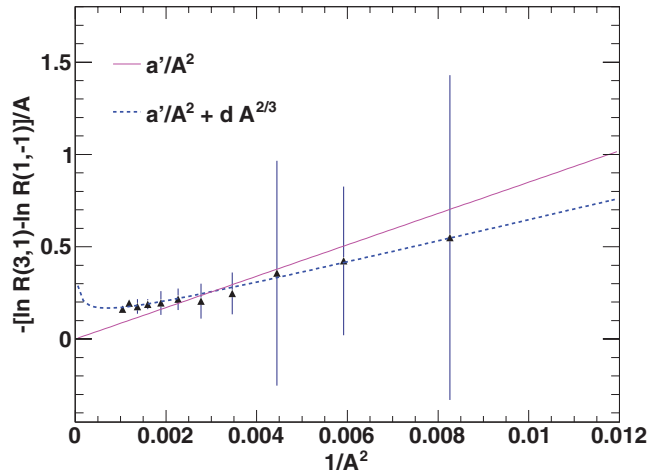

FIG. 7. (Color online) Quantity $-[\ln R(3,1) - \ln R(1,-1)]/A^2$ vs $1/A^2$ calculated from isobaric yield ratios for an average source isospin asymmetry $\overline{m_s} = 0$. The dashed and full lines are the best fits to the data with a first-degree function, including and not including the Coulomb contribution, respectively.

The parameters, evaluated for all possible m_s and excitation energy combinations, are plotted in Fig. 6. The best fit and the line representing $\alpha = -\beta$ are also plotted in the figure. The relation $\alpha = -\beta$ appears to be approximately satisfied in our data ($-\beta = 1.11\,\alpha$), thus supporting the equivalence of the isoscaling and the m-scaling. Therefore we can use Eq. (7) to calculate $\frac{C_{\rm sym}}{T}$ from m-scaling, using $\alpha = \Delta H/T$. Small differences between α and $-\beta$ might be attributed to residual Coulomb effects. Indeed, although the ratio of the yields of a single isotope is considered, the two sources, whose m_s is fixed, might have different charges. We remind the reader that the *SumZ* selection constrains the source charge to be $Z = 25$–30.

The residual Coulomb effect due to differences in the charge of the considered fragments is relevant only in the calculation of $\frac{C_{\rm sym}}{T}$ by the isobaric yield ratio method and it influences mainly large mass fragments. From the mass formula the Coulomb energy for large Z can be written as [33]

$$\frac{E_c}{A} = 0.77\frac{Z^2}{A^2}A^{2/3} = \frac{0.77}{4}(1-m)^2A^{2/3}. \qquad (16)$$

Adding this term to the free energy Ψ/T in Eq. (5), we see that a quadratic and a linear term in m are introduced that modify the symmetry energy coefficient and the external field. Also a term not dependent on m is introduced. The effect of introducing such corrections is extensively discussed in Ref. [33]. Here we concentrate on evaluating the Coulomb contribution, as well as the importance of $o(m^4)$ and $o(m^6)$ terms in Eq. (5). First of all we should notice that, assuming a spherical expansion, at low densities the Coulomb energy decreases as $\rho^{1/3}$. A fit of the quantity $-[\ln R(3,1) - \ln R(1,-1)]/A^2$ allows us to estimate the fitting parameters of Eq. (5) and the Coulomb term. The fit results are shown in Fig. 7. The dashed and full lines are the best fit to the data with a first-degree polynomial of $1/A^2$ including and not including the Coulomb correction, respectively. We remind the reader that $(1/A^2) \propto m^2$. The parameters a' and d are fitting parameters. We found that $o(m^4)$ terms are negligible, since we are dealing with relatively large fragments, which implies small m (but possibly large Coulomb effects). The Coulomb parameter d is about two orders of magnitude smaller than the $1/A^2$ coefficient a', but the term has to be included in the fitting function to obtain a good fit (χ^2/degrees of freedom ≈ 0.8). We therefore took into account this correction and modified Eq. (13) as

$$\frac{C_{\rm sym}(T)}{T} \approx -\frac{A}{8}[\ln R(3,1,A) - \ln R(1,-1,A) - \delta(3,1,A)] - d\,A^{2/3}. \qquad (17)$$

The α parameters are related to $\frac{C_{\rm sym}}{T}$ through the value of Δ, as given in Eq. (7). Therefore, the extracted value of the symmetry term depends on the choice of Δ. The isobaric yield ratio method instead provides a $\frac{C_{\rm sym}}{T}$ value independent of the choice of Δ. Three different definitions of Δ have been examined. The Z/A of the emitting source has been adopted for the definition of $\Delta_{\rm source}$ [Eq. (8)]. The average proton content of each fragment with mass greater than 4 has been used to calculate $\Delta_{\rm liquid}$ [Eq. (9)]. Finally, the average of the fragment $\langle\overline{m_f}\rangle$ over the events has been used to define $\Delta_{\langle m_f\rangle}$ [Eq. (10)]. The three different Δ values as a function of the fragment charge for a given $\Delta\overline{m_s}$ and excitation energy combination are plotted in Fig. 8. By definition, $\Delta_{\rm source}$ (red, dashed curve) and $\Delta_{\langle m_f\rangle}$ (black, full curve) are independent of Z. We observe that $\Delta_{\langle m_f\rangle} \approx 0.3\Delta_{\rm source}$, which is close to the value reported in Ref. [37]. The large discrepancy between the value of $\Delta_{\rm source}$ and the values of $\Delta_{\rm liquid}$ and $\Delta_{\langle m_f\rangle}$ is due to the fact that, while both $\Delta_{\rm liquid}$ and $\Delta_{\langle m_f\rangle}$ are related to the fragment composition, $\Delta_{\rm source}$ is related to the source composition. The quantity $\Delta_{\rm liquid}$ (asterisks) shows an odd-even behavior for $Z \leqslant 8$, which can be attributed to structure effects [49]. Such an odd-even effect is in agreement with the trend reported in [49–51]. The overall behavior shows a rather significant decrease as a function of Z, which will cause $\frac{C_{\rm sym}}{T}$ to increase as a function of Z. The very high value of $\Delta_{\rm liquid}$ for Be is due to the fact that ^{8}Be, produced

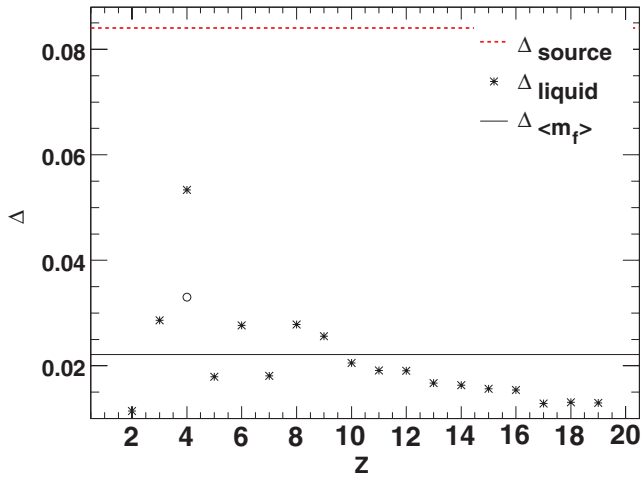

FIG. 8. (Color online) Values of Δ computed according to the different definitions of Eqs. (8), (9), and (10) vs the fragment charge Z for $\Delta\overline{m_s} = 0.185$ and $3.5 \leqslant E_t^\star/A \leqslant 5$ MeV.

in the multifragmentation process, decays before reaching the detector, and thus $\langle A\rangle$ deviates from the "true" centroid of the isotope distribution. An attempt was made to estimate the ^{8}Be yield from the $N = Z$ nuclei yields, whose corrected value is plotted in the figure as a circle. A plot of the yield versus mass number for $m_f = 0$ fragments displays a power-law behavior with $Y \propto A^{-\tau}$ [33]. The yield of ^{8}Be has been estimated from a fit of $CA^{-\tau}$ to the data for even-even $N = Z$ nuclei, for which the pairing contribution is the same. The value of Δ changes from 0.053 to 0.033.

Figure 9 shows a comparison between the three methods, with different choices of Δ, for a given excitation energy [$3.5 \leqslant E_t^\star/A < 5.0$ MeV; panels (a)–(c)] and for a given source asymmetry difference [$\Delta\overline{m_s} = 0.086$; panels (a) and (d)–(f)]. The $\frac{C_{\rm sym}}{T}$ values obtained by the isobaric yield ratio method (triangles) show an approximately constant behavior for $A < 20$, while an increase is observed for $A = 21$ and 23. This is observed for all the $\Delta\overline{m_s}$ combinations and excitation energy windows. The observed increase of 3–4 units in $\frac{C_{\rm sym}}{T}$ for A from 11 to 23 is smaller than the increase observed in Ref. [18]. We would like to emphasize that one of the main limitations of the isobaric yield ratio method is that it requires a nearly "ideal" isotopic identification, since any contamination by other isotopes to each (Z, A) fragment affects different isobars by a different amount. This effect is particularly relevant for the yield estimate of heavy particles. Indeed, the mass resolution decreases with increasing fragment size (see Fig. 1), lowering the particle identification efficiency. While this effect largely cancels out when the yield ratio of the same fragment produced by two different sources is taken (i.e., isoscaling and m-scaling), the $\frac{C_{\rm sym}}{T}$ estimation for the isobaric yield ratio method remains affected. For this reason, data for $A \geqslant 25$, when available, are not shown for the isobaric yield ratio method, while they are presented for the isoscaling and m-scaling methods. Indeed, we do not observe a change of behavior of α as a function of A extracted from the isoscaling and m-scaling methods even in the high-mass region (see Fig. 3).

The trends of $\frac{C_{\rm sym}}{T}$ obtained from the isoscaling and m-scaling depend on the definition of Δ, as discussed in relation to Eq. (7). First, we notice that $\frac{C_{\rm sym}}{T}$ obtained from the isoscaling with the three definitions of Δ are not in agreement. This is due to the differences in the values of Δ, which is clearly shown in Fig. 8. The $\frac{C_{\rm sym}}{T}$ values determined using $\Delta_{\rm source}$ (crosses) and $\Delta_{\langle m_f\rangle}$ (circles) do not show any A dependence, while a clearly increasing trend is observed for $A > 15$ for values determined using $\Delta_{\rm liquid}$ (squares). This is caused by the dependence of $\Delta_{\rm liquid}$ on A, as shown in Fig. 8. For $A < 15$ the structure effects affecting $\Delta_{\rm liquid}$ are reflected in $\frac{C_{\rm sym}}{T}$ values.

The $\frac{C_{\rm sym}}{T}$ values determined using $\Delta_{\langle m_f\rangle}$ from the isoscaling (full circles) and m-scaling (open circles) show a generally good agreement for all the $\Delta\overline{m_s}$ combinations. We can see that the values obtained from the m-scaling are systematically higher than those obtained from the isoscaling, which could be due to the residual Coulomb effects noted above. The difference decreases as the excitation energy increases, as can be seen comparing Figs. 9(a), 9(d), 9(e), and 9(f).

Comparing Figs. 9(a)–9(c), we observe that the values obtained with the isoscaling and m-scaling, using $\Delta_{\langle m_f\rangle}$, do not depend on the choice of $\Delta\overline{m_s}$. Indeed, the weighted average values (10.19 ± 0.04, 10.10 ± 0.20, and 10.12 ± 0.16 and 9.22 ± 0.05, 8.90 ± 0.20, and 9.07 ± 0.15 for $\Delta\overline{m_s} = 0.086$, 0.180, and 0.279 and extracted by m-scaling and isoscaling, respectively) are consistent within 2σ. The increase in the uncertainties reflects the decrease of available statistics as the considered m_s bins are further apart, i.e., when we consider the tails of the m_s distribution (see Fig. 2).

An excitation energy dependence of $\frac{C_{\rm sym}}{T}$ can be extrapolated from Figs. 9(a) and 9(d)–9(f): $\frac{C_{\rm sym}}{T}$ decreases from 11.1(±0.08) to 7.7(±0.04) as the source excitation energy increases. This trend is observed for the $\Delta_{\langle m_f\rangle}$ derived quantities, as well as for $\frac{C_{\rm sym}}{T}$ derived with the other Δ definitions. As already discussed, this trend is in agreement with the excitation energy dependence of the isoscaling parameter α/Δ observed in [40]. An excitation energy dependence of $\frac{C_{\rm sym}}{T}$ is also observed for the m-scaling extracted quantities, which vary from 12.47(±0.08) to 8.20(±0.04), increasing the excitation energy. In contrast, a weaker excitation energy dependence is found for the values extracted with the isobaric yield ratio method, which decreases from 10.0(±0.4) to 8.8(±0.2), increasing the excitation energy.

We now compare the values obtained with the different Δ definitions to the values extracted from the isobaric yield ratio, since they are independent of the choice of Δ. The $\frac{C_{\rm sym}}{T}$ values determined using $\Delta_{\rm source}$ (crosses) are lower than those determined with the isobaric yield ratio method (triangles) by a factor 2 to 3 independent of Δm_s and independent of the excitation energy. The $\frac{C_{\rm sym}}{T}$ values determined using $\Delta_{\rm liquid}$ (squares) show a rather good agreement for $A \approx 18$–22 in the central mass region, where $\Delta_{\rm liquid} \approx \Delta_{\langle m_f\rangle}$. Nevertheless, it does not reproduce the data for the low-mass region, where structure effects influence the value of $\Delta_{\rm liquid}$, as pointed out in Fig. 8. In this region, in contrast to the high-mass region, the isotopic resolution of each fragment is very good and presents

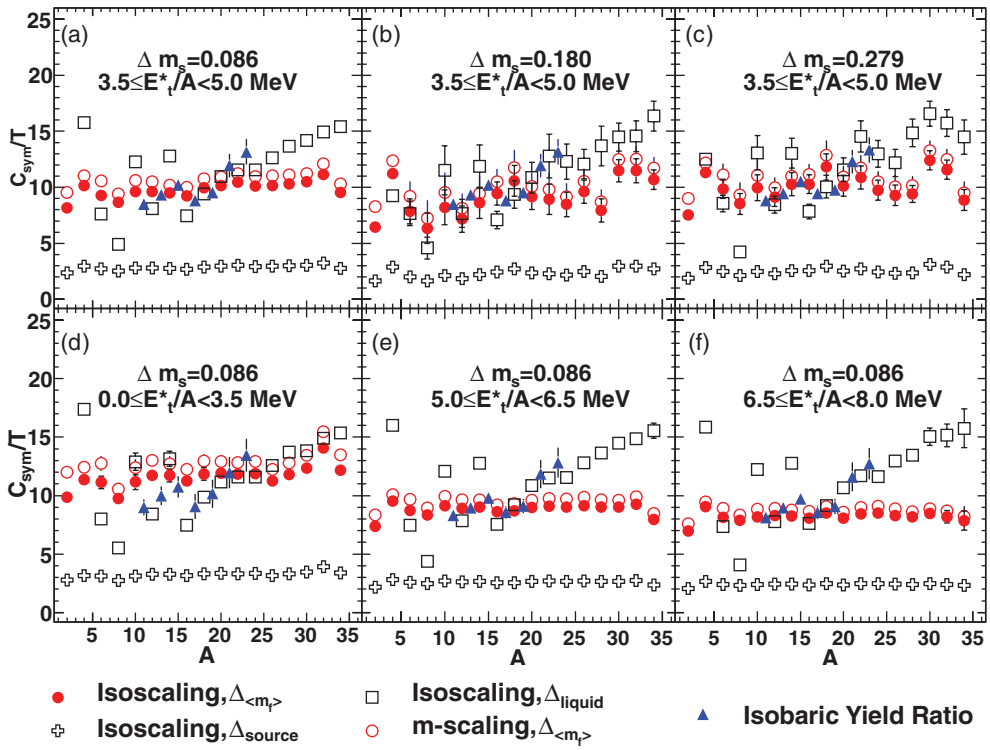

FIG. 9. (Color online) Values of $\frac{C_{\rm sym}}{T}$ obtained with the three different methods. Each panel corresponds to the noted $\Delta\overline{m_s}$ and the noted window in $E_t^\star/A$. Three different choices of Δ have been used to compute $\frac{C_{\rm sym}}{T}$ from the isoscaling parameter α.

a small uncertainty; thus, we have confidence in the extracted $\frac{C_{\rm sym}}{T}$ values. The $\frac{C_{\rm sym}}{T}$ values determined using $\Delta_{\langle m_f\rangle}$, both from isoscaling and m-scaling, show good agreement with the isobaric yield ratio values for masses up to $A \approx 20$, for all the $\Delta\overline{m_s}$ and excitation energy combinations. This is consistent with what was recently observed by Tripathi *et al.* [37]. In this work the authors show that the position of the free energy central minimum, when an external field is present (i.e., when $m_s \neq 0$ [17]), is related to $\langle\overline{m_f}\rangle$ rather than to m_s. This indicates that the connection between quantities extracted from fragment yields and the symmetry energy coefficient has to be found in the composition of the emitted fragments, taking into account the event multiplicity.

The generally flat behavior of $\frac{C_{\rm sym}}{T}$ as a function of A (circles and triangles in Fig. 9) may be interpreted as the weak influence of secondary decay effects on the observables. This in turn implies that fragments are determined in the instability region in agreement with the theoretical work of Dorso and Randrup [52]. This would also be the case in a first-order phase transition for infinite nuclei, where the size of a cluster is determined by its internal pressure, which takes into account the surface tension, and the external pressure due to the gas [34]. For finite systems the formed fragments might reach the ground state by emitting low-energy γ rays and possibly a neutron. Also the constancy of $\frac{C_{\rm sym}}{T}$ might indicate that the assumption of constant volume is reasonable and we can identify this quantity as the symmetry energy rather than the enthalpy.

VII. CONCLUSIONS

Three methods to extract the symmetry energy coefficient from fragment yields were compared. The isobaric yield ratio method removes the dependence on the fragmenting source by computing the difference of the yield ratios of properly chosen isobars produced by the same source, but the dependence on individual isobar detection efficiencies remains. The m-scaling and the isoscaling, however, retain a dependence on the source characteristics in the difference of the external fields of the two sources ($\Delta H/T$), while significantly reducing the dependence on isotopic detection efficiencies. The determination of $\frac{C_{\rm sym}}{T}$ in this case depends on the choice of Δ.

The symmetry energy coefficient to temperature ratio, $\frac{C_{\rm sym}}{T}$, was experimentally evaluated as a function of the fragment mass with the three different methods. The effect of the source reconstruction on the $\frac{C_{\rm sym}}{T}$ values was analyzed, showing that 4π angular coverage is useful in extracting information from the isobaric yield ratios, since a limited coverage impacts $\frac{C_{\rm sym}}{T}$ values. Improved isoscaling and m-scaling were observed when selecting quasiprojectile m_s bins for neutron-rich and neutron-poor systems, while isobaric-yield-ratio-extracted values were only slightly affected. A decrease in $\frac{C_{\rm sym}}{T}$ was observed with increasing excitation energy.

The isoscaling parameters α and β were extracted as a function of Z for all m_s and excitation energy combinations. Our data show the equivalence of the isoscaling and the m-scaling, since the relation $\alpha = -\beta$ is approximately satisfied.

The $\frac{C_{\rm sym}}{T}$ values extracted from the α isoscaling parameter using $\Delta_{\langle m_f \rangle}$ are in good agreement with the isobaric yield ratio $\frac{C_{\rm sym}}{T}$ values. This indicates that the connection between α and $\frac{C_{\rm sym}}{T}$ has to be found in the average fragment isotopic asymmetry. The extracted symmetry term shows a generally flat trend as a function of A for the mass region $A = 10$–20 with the best mass resolution, independent of the method used. This may be consistent with the lack of secondary de-excitation effects in our data, within our isotopic resolution, as well as with the assumption of a freeze-out volume where the disassembly occurs.

ACKNOWLEDGMENTS

This work was supported by US Department of Energy Grant No. DE-FG03-93ER40773 and the Robert A. Welch Foundation Grant No. A-1266.

[1] B. A. Brown, Phys. Rev. Lett. **85**, 5296 (2000).
[2] J. M. Lattimer and M. Prakash, Astrophys. J. **550**, 426 (2001).
[3] L. Trippa, G. Colò, and E. Vigezzi, Phys. Rev. C **77**, 061304 (2008).
[4] A. Klimkiewicz *et al.*, Phys. Rev. C **76**, 051603 (2007).
[5] T. Li, U. Garg *et al.*, Phys. Rev. Lett. **99**, 162503 (2007).
[6] M. A. Famiano *et al.*, Phys. Rev. Lett. **97**, 052701 (2006).
[7] M. B. Tsang *et al.*, Phys. Rev. Lett. **92**, 062701 (2004), and references therein.
[8] M. B. Tsang, W. A. Friedman, C. K. Gelbke, W. G. Lynch, G. Verde, and H. S. Xu, Phys. Rev. Lett. **86**, 5023 (2001).
[9] J. Iglio, D. V. Shetty, S. J. Yennello, G. A. Souliotis, M. Jandel, A. L. Keksis, S. N. Soisson, B. C. Stein, S. Wuenschel, and A. S. Botvina, Phys. Rev. C **74**, 024605 (2006).
[10] R. C. Lemmon and P. Russotto for the ASY-EOS Collaboration, Constraining the symmetry energy at supra-saturation densities with measurements of neutron and proton elliptic flows, Experiment proposal at GSI.
[11] H. S. Xu *et al.*, Phys. Rev. Lett. **85**, 716 (2000).
[12] M. B. Tsang *et al.*, Phys. Rev. C **64**, 054615 (2001).
[13] A. S. Botvina, O. V. Lozhkin, and W. Trautmann, Phys. Rev. C **65**, 044610 (2002).
[14] A. Ono, P. Danielewicz, W. A. Friedman, W. G. Lynch, and M. B. Tsang, Phys. Rev. C **68**, 051601(R) (2003).
[15] G. A. Souliotis, M. Veselsky, D. V. Shetty, and S. J. Yennello, Phys. Lett. B **588**, 35 (2004).
[16] A. Le Fèvre *et al.*, Phys. Rev. Lett. **94**, 162701 (2005).
[17] M. Huang *et al.*, Nucl. Phys. A **847**, 233 (2010).
[18] M. Huang *et al.*, Phys. Rev. C **81**, 044620 (2010).
[19] A. Bonasera, F. Gulminelli, and J. Molitoris, Phys. Rep. **243**, 1 (1994).
[20] A. Bonasera, M. Bruno, C. O. Dorso, and P. F. Mastinu, Riv. Nuovo Cimento **23**, 1 (2000).
[21] B. Borderie and M. F. Rivet, Prog. Part. Nucl. Phys. **61**, 551 (2008).
[22] W. Trautmann, Nucl. Phys. A **752**, 407 (2005).
[23] S. Kowalski *et al.*, Phys. Rev. C **75**, 014601 (2007).
[24] R. W. Minich, S. Agarwal, A. Bujak, J. Chuang, J. E. Finn, L. J. Gutay, A. S. Hirsch, N. T. Porile, R. P. Scharenberg, B. C. Stringfellow, and F. Turkot, Phys. Lett. B **118**, 458 (1982).
[25] M. Belkacem, V. Latora, and A. Bonasera, Phys. Rev. C **52**, 271 (1995).
[26] A. Ono, P. Danielewicz, W. A. Friedman, W. G. Lynch, and M. B. Tsang, Phys. Rev. C **70**, 041604(R) (2004).
[27] C. B. Das, S. Das Gupta, W. G. Lynch, A. Z. Mekjian, and M. B. Tsang, Phys. Rep. **406**, 1 (2005).
[28] J. P. Bondorf, A. S. Botvina, A. S. Iljinov, I. N. Mishustin, and K. Sneppen, Phys. Rep. **257**, 133 (1995).
[29] Z. Chen *et al.*, Phys. Rev. C **81**, 064613 (2010).
[30] L. G. Sobotka, Phys. Rev. C **84**, 017601 (2011).
[31] G. A. Souliotis, D. V. Shetty, A. Keksis, E. Bell, M. Jandel, M. Veselsky, and S. J. Yennello, Phys. Rev. C **73**, 024606 (2006).
[32] S. Galanopoulos, G. A. Souliotis, A. L. Keksis, M. Veselsky, Z. Kohley, L. W. May, D. V. Shetty, S. N. Soisson, B. C. Stein, S. Wuenschel, and S. J. Yennello, Nucl. Phys. A **837**, 145 (2010).
[33] M. Huang *et al.*, Phys. Rev. C **81**, 044618 (2010).
[34] K. Huang, *Statistical Mechanics* (Wiley, New York, 1987), 2nd ed., Chaps. 16 and 17.
[35] A. Bonasera, Z. Chen, R. Wada, K. Hagel, J. Natowitz, P. Sahu, L. Qin, S. Kowalski, Th. Keutgen, T. Materna, and T. Nakagawa, Phys. Rev. Lett. **101**, 122702 (2008).
[36] A. Ono, H. Horiuchi, T. Maruyama, and A. Ohnishi, Phys. Rev. Lett. **68**, 2898 (1992).
[37] R. Tripathi *et al.*, arXiv:1010.2227.
[38] C. F. Weizsäcker, Z. Phys. **96**, 431 (1935).
[39] H. A. Bethe, Rev. Mod. Phys. **8**, 82 (1936).
[40] S. Wuenschel *et al.*, Phys. Rev. C **79**, 061602(R) (2009).
[41] N. Marie *et al.*, Phys. Rev. C **58**, 256 (1998).
[42] S. Hudan *et al.*, Phys. Rev. C **67**, 064613 (2003).
[43] Z. Kohley, Ph.D. thesis, Texas A&M University, 2010.
[44] S. Wuenschel *et al.*, Nucl. Instrum. Methods Phys. Res., Sect. A **604**, 578 (2009).
[45] S. Wuenschel, K. Hagel, L. W. May, R. Wada, and S. J. Yennello, AIP Conf. Proc. **1099**, 816 (2009).
[46] J. C. Steckmeyer *et al.*, Nucl. Phys. A **686**, 537 (2001).
[47] S. Wuenschel *et al.*, Nucl. Phys. A **843**, 1 (2010); S. Wuenschel, Ph.D. thesis, Texas A&M University, 2009.
[48] D. Doré *et al.*, Phys. Lett. B **491**, 15 (2000).
[49] E. M. Winchester, J. A. Winger, R. Laforest, E. Martin, E. Ramakrishnan, D. J. Rowland, A. Ruangma, S. J. Yennello, G. D. Westfall, A. Vander Molen, and E. Norbeck, Phys. Rev. C **63**, 014601 (2000).
[50] E. Martin, R. Laforest, E. Ramakrishnan, D. J. Rowland, A. Ruangma, E. M. Winchester, and S. J. Yennello, Phys. Rev. C **62**, 027601 (2000).
[51] D. V. Shetty *et al.*, Phys. Rev. C **68**, 054605 (2003).
[52] C. Dorso and J. Randrup, Phys. Lett. B **301**, 328 (1993).